Nonlinear Dyn (2010) 59: 207–219
DOI 10.1007/s11071-009-9533-9

ORIGINAL PAPER

Nonlinear dynamic response of a functionally graded plate with a through-width surface crack

J. Yang · Y.X. Hao · W. Zhang · S. Kitipornchai

Received: 4 February 2009 / Accepted: 14 May 2009 / Published online: 30 May 2009

Abstract A nonlinear vibration analysis of a simply supported functionally graded rectangular plate with a through-width surface crack is presented in this paper. The plate is subjected to a transverse excitation force. Material properties are graded in the thickness direction according to exponential distributions. The cracked plate is treated as an assembly of two subplates connected by a rotational spring at the cracked section whose stiffness is calculated through stress intensity factor. Based on Reddy's third-order shear deformation plate theory, the nonlinear governing equations of motion for the FGM plate are derived by using the Hamilton's principle. The deflection of each subplate is assumed to be a combination of the first two mode shape functions with unknown constants to be determined from boundary and compatibility conditions. The Galerkin's method is then utilized to convert the governing equations to a two-degree-of-freedom nonlinear system including quadratic and cubic nonlinear terms under the external excitation, which is numerically solved to obtain the nonlinear responses of cracked FGM rectangular plates. The influences of material property gradient, crack depth, crack location and plate thickness ratio on the vibration frequencies and transient response of the surface-racked FGM plate are discussed in detail through a parametric study.

Keywords Functionally graded materials · Rectangular plate · Nonlinear dynamic response · Surface crack · Third-order shear deformation plate theory

J. Yang (✉)
School of Aerospace, Mechanical and Manufacturing Engineering, RMIT University, P.O. Box 71, Bundoora, VIC 3083, Australia
e-mail: j.yang@rmit.edu.au

Y.X. Hao · W. Zhang
College of Mechanical Engineering, Beijing University of Technology, Beijing 100022, P.R. China

S. Kitipornchai
Department of Building and Construction, City University of Hong Kong, Kowloon, Hong Kong

1 Introduction

Functionally graded materials (FGMs) are advanced composites with continuously varying material composition and properties from one surface to another. This eliminates the mismatch between thermal and mechanical properties at the interface between two distinct materials. FGMs have been receiving increasing attention in both research community and industry due to their excellent thermomechanical properties [1]. Nonlinear dynamic behavior of FGM structures has been a subject area of extensive research efforts and quite a few investigations have been conducted. Among many others, Praveen and Reddy [2]

analyzed the nonlinear transient response of FGM plates subjected to a steady temperature field together with a lateral dynamic load by using the first-order shear deformation plate theory and the finite element method. Reddy [3] developed both theoretical and finite element formulations for thick FGM plates according to third-order shear deformation plate theory, and studied the nonlinear dynamic response of FGM plates subjected to a suddenly applied uniform pressure. Yang et al. [4] presented large-amplitude vibration analysis of pre-stressed FGM laminated plates composed of an FGM layer and two surface-mounted piezoelectric actuator layers. Huang and Shen [5] dealt with the nonlinear vibration and dynamic response of FGM plates undergoing one-dimensional steady heat conduction in thickness direction and considered temperature-dependent material properties. Chen [6] investigated the effect of initial in-plane stresses on the nonlinear vibration of FGM plates. More recently, Yang and his coworkers studied the sensitivity of nonlinear vibration and dynamic response of FGM plates to initial geometrical imperfections of arbitrary shape [7, 8].

It is well known that the presence of crack defects in a structure introduces a local flexibility, reduces the stiffness and may change the dynamic behavior of the structure. An in-depth understanding of the dynamic characteristics of cracked structures is of prime importance in structural health monitoring and reliability assessment because the predicted vibration data can be used to detect, locate, and quantify the extent of the cracks or damages in a structure [9]. Literature review shows that although there are quite a few papers concerning the crack and fracture analyses of FGM structures [10–16], the investigations concerning the effect of crack defects on the dynamic behavior of FGM structures are still very limited in number. Sridhar et al. [17] developed an effective pseudo-spectral finite element method for wave propagation analysis in anisotropic and inhomogeneous structures with or without vertical and horizontal cracks. They also demonstrated the effectiveness of modulated pulse in detecting small cracks in composites and FGMs. Birman and Byrd [18] examined free and forced vibration of a functionally graded cantilever beam with damages such as a region with degraded stiffness adjacent to the root of the beam, a single delamination crack, and a single crack at the root of cross section of the beam propagating in the thickness direction. Yang and Chen [19] analytically investigated the influence of open edge cracks on the vibration and buckling of Euler–Bernoulli FGM beams with different boundary conditions. They also studied the free and forced vibration of cracked Euler–Bernoulli inhomogeneous beams under an axial force and a transverse moving load [20]. Ke et al. [21] obtained analytical solutions for the natural frequencies and elastic buckling load of cracked FGM Timoshenko beams under three different end supports. It is noted that the above-mentioned studies [17–21] dealt with linear vibration of cracked FGM beams and plates only, no previous work has so far been conducted to investigate the nonlinear vibration behavior of cracked FGM structures, which is an important topic deserving special attention especially when the FGM structure is subjected to large dynamic loads.

This paper attempts to study the nonlinear vibration of a simply supported FGM rectangular plate containing a through-width surface crack subjected to a transverse excitation force. The material composition varies exponentially in the thickness direction. Theoretical formulations are based on Reddy's third-order shear deformation plate theory [3, 22] to account for the effect of transverse shear deformation, von Karman nonlinear kinematics to include the large deflection and the rotational spring model to treat the cracked plate as an assembly of two sub-plates connected by a rotation spring at the cracked section. The stiffness of the cracked section is calculated via the stress intensity factor. The governing equations of motion, which are derived by using the Hamilton's principle, are reduced to a two-degree-of-freedom nonlinear system by employing the Galerkin's method. A parametric study is then carried out to gain an insight into the influences of material property gradient, crack parameters, and plate thickness ratio on the linear and nonlinear vibration of cracked FGM plates. It should be mentioned that the present analysis can also be extended to FGM plates with other material property distributions such as simple power law. This can easily be done by using the associated distribution functions in (1) and the stress intensity factor in (3) in theoretical formulations.

2 Theoretical formulations

Consider a simply supported rectangular FGM plate ($a \times b \times h$) containing a through-width surface crack

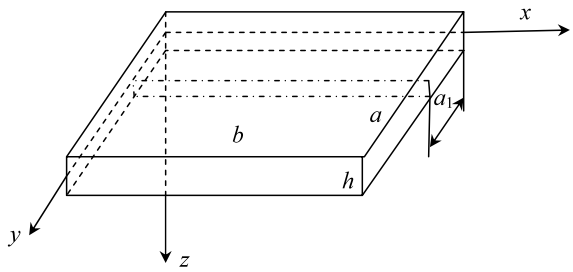

Fig. 1 An FGM rectangular plate with a through-width surface crack

parallel to the x-axis located at a distance of a_1 from the edge $y = 0$ with crack depth h_1, as shown in Fig. 1. The plate is defined in a Cartesian coordinate $Oxyz$, where (x, y) are the coordinates of a point in the mid-plane $(z = 0)$ of the plate and z is perpendicular to the mid-plane and points downwards. It is assumed that the shear modulus ν, the Young's modulus E, and the mass density ρ of the plate vary in the thickness direction only, following exponential distributions:

$$\nu(z) = \nu_0 e^{\beta z}, \qquad E(z) = E_0 e^{\beta z}, \qquad \rho(z) = \rho_0 e^{\beta z}, \tag{1}$$

where ν_0, E_0 and ρ_0 are the shear modulus, the Young's modulus and the mass density at the mid-plane of the plate; constant β describes material property gradient along the thickness direction. As a special case, $\beta = 0$ indicates an isotropic homogeneous plate. Poisson's ratio μ is taken as a constant in the analysis since its effect on the stress intensity factors is negligible [11]. It is assumed that the crack is perpendicular to the plate surface and always remains open. Based on the well accepted rotational-spring model, the cracked plate can be treated as two sub-plates connected by an elastic rotational spring at the cracked section which has no mass and no length. The bending stiffness of the cracked section k_τ is related to the flexibility G by

$$k_\tau = \frac{1}{G}. \tag{2}$$

From Broek's approximation [23], the flexibility G due to the presence of the crack can be derived as

$$\frac{(1-\mu^2)K_{\mathrm{I}}^2}{E(z)} = \frac{M_{\mathrm{I}}^2}{2}\frac{dG}{da}, \tag{3}$$

where M_I is the bending moment at the cracked section, K_I is the stress intensity factor (SIF) under mode I loading and is a function of the geometry, loading, and material properties. For an FGM strip with an open edge crack under bending, the expression of SIF was given by Erdogan and Wu [11].

Suppose the plate is subjected to a transverse excitation force $q(x, y, t)$ with excitation frequency Ω. Let (u, v, w) be the displacements of an arbitrary point within the plate in the x-, y-, and z-axes, (u_0, v_0, w_0) be the mid-plane displacement components, ϕ_x and ϕ_y denote the slope rotations in the x–z and y–z planes, respectively. In accordance with Reddy's third-order shear deformation plate theory [3, 22], the displacement field of an arbitrary point within the plate domain is

$$u(x, y, z, t) = u_0(x, y, t) + z\phi_x(x, y) - c_1 z^3\left[\phi_x(x, y, t) + \frac{\partial w(x, y, t)}{\partial x}\right], \tag{4a}$$

$$v(x, y, z, t) = v_0(x, y, t) + z\phi_y(x, y, t) - c_1 z^3\left[\phi_y(x, y, t) + \frac{\partial w(x, y, t)}{\partial y}\right], \tag{4b}$$

$$w(x, y, z, t) = w_0(x, y, t), \tag{4c}$$

where $c_1 = 4/3h^2$,

Within the framework of von Karman nonlinear kinematics, the governing equations of motion for each sub-plate can be derived by using Hamilton's principle and expressed in terms of displacement components $u_0, v_0, w_0, \phi_x, \phi_y$ as

$$L_{jL}\left(u_0^i, v_0^i, w_0^i, \phi_x^i, \phi_y^i\right) = L_{jR}\left(\ddot{u}_0^i, \ddot{v}_0^i, \ddot{w}_0^i, \ddot{\phi}_x^i, \ddot{\phi}_y^i\right) \tag{5}$$

where superscripts $i = 1, 2$ refer to the two sub-plates divided by the cracked section. The nonlinear partial differential operators L_{jL} $(j = 1, \ldots, 5)$ and linear partial differential operators L_{jR} $(j = 1, \ldots, 5)$ are given in Appendix. The stiffness elements of the FGM plate are defined by

$$(A_{ij}, B_{ij}, D_{ij}, E_{ij}, F_{ij}, H_{ij}) = \int_{-h/2}^{h/2} Q_{ij}\left(1, z, z^2, z^3, z^4, z^6\right) dz \quad (i, j = 1, 2, 6), \tag{6a}$$

$$(A_{ij}, D_{ij}, F_{ij}) = \int_{-h/2}^{h/2} Q_{ij}\left(1, z^2, z^4\right) dz \quad (i, j = 4, 5), \tag{6b}$$

where the elastic stiffnesses are position-dependent and are given by

$$Q_{11} = Q_{22} = \frac{E}{1-\mu^2}, \qquad Q_{12} = Q_{21} = \frac{\mu E}{1-\mu^2}, \qquad Q_{44} = Q_{55} = Q_{66} = \frac{E}{2(1+\mu)}, \tag{7}$$

the inertia-related terms are calculated from

$$I_i = \int_{-h/2}^{h/2} z^i \rho(z)\, dz \quad (i = 0, 1, 2, 3, 4, 6). \tag{8}$$

The boundary conditions for the simply supported cracked FGM plate requires that

$$w_0^1 = \phi_y^1 = M_{xx}^1 = P_{xx}^1 = N_{xy}^1 = N_{xx}^1 = 0 \quad (x = 0, b) \tag{9a}$$

$$w_0^1 = \phi_x^1 = M_{yy}^1 = P_{yy}^1 = N_{xy}^1 = N_{yy}^1 = 0 \quad (y = 0) \tag{9b}$$

for the first sub-plate, and

$$w_0^2 = \phi_y^2 = M_{xx}^2 = P_{xx}^2 = N_{xy}^2 = N_{xx}^2 = 0 \quad (x = 0, b) \tag{10a}$$

$$w_0^2 = \phi_x^2 = M_{yy}^2 = P_{yy}^2 = N_{xy}^2 = N_{yy}^2 = 0 \quad (y = a) \tag{10b}$$

for the second sub-plate, where (N_{xx}, N_{xy}, N_{yy}), (M_{xx}, M_{xy}, M_{yy}), and (P_{xx}, P_{xy}, P_{yy}) are stress resultants, bending moments and higher-order moments defined in [3, 22].

At the cracked section $(y = a_1)$, the compatibility condition enforces continuities in all displacement components, force resultants and bending moments, except for ϕ_y which is discontinuous and exhibits a jump that is proportional to the bending moment transmitted, i.e.

$$w_0^1 = w_0^2, \quad u_0^1 = u_0^2, \quad v_0^1 = v_0^2, \quad \phi_x^1 = \phi_x^2, \quad N_{yy}^1 = N_{yy}^2, \quad P_{yy}^1 = P_{yy}^2, \tag{11a}$$

$$\kappa_\tau\left(\phi_y^1 - \phi_y^2\right) = M_{yy}^1. \tag{11b}$$

Following the work by Bhimaraddi [24] and Nosir and Reddy [25] to neglect the in-plane and rotary inertia terms in (5) since their influences are small compared to the transverse inertia term, one can obtain from the 1st, 2nd, 4th and 5th equations in (5) the expressions of u_0^i, v_0^i, ϕ_x^i and ϕ_y^i in terms of w_0^i. These expressions are then substituted into the 3rd equation in (5) to convert it into a partial differential equation in w_0^i only. The present study focuses on the nonlinear transverse oscillations of surface-cracked FGM plates in the first two modes. It is then reasonable to construct deflection functions as a combination of the first two vibration mode shapes as below:

$$w_0^1 = w_1 \sin\left(\frac{\pi x}{b}\right)\left[\sin\left(\frac{3\pi y}{a}\right) + \delta_{11}\sin\left(\frac{3\pi y}{a_1}\right)\right] + w_2 \sin\left(\frac{3\pi x}{b}\right) \times \left[\sin\left(\frac{\pi y}{a}\right) + \delta_{13}\sin\left(\frac{\pi y}{a_1}\right)\right], \tag{12a}$$

$$w_0^2 = w_1 \sin\left(\frac{\pi x}{b}\right)\left[\sin\left(\frac{3\pi y}{a}\right) + \delta_{21}\sin\left(\frac{3\pi(a-y)}{a-a_1}\right)\right] + w_2 \sin\left(\frac{3\pi x}{b}\right) \times \left[\sin\left(\frac{\pi y}{a}\right) + \delta_{23}\sin\left(\frac{\pi(a-y)}{a-a_1}\right)\right], \tag{12b}$$

where w_1 and w_2 are the time-varying vibration amplitudes of the first two modes. The constants $\delta_{11}, \delta_{13}, \delta_{21}$ and δ_{23} are to be determined from boundary conditions in (9) and (10) and the compatibility condition at the cracked section in (11) by using the Least Squares technique.

The transverse excitation force can be represented by

$$q(x, y, t) = F_1(t)\sin\frac{\pi x}{b}\sin\frac{3\pi y}{a} + F_2(t)\sin\frac{3\pi x}{b}\sin\frac{\pi y}{a}, \tag{13}$$

where F_1 and F_2 are the amplitudes of the transverse forcing functions.

Finally, substituting (12) and (13) into the 3rd equation in (5) expressed in terms of w_0^i only and applying

the Galerkin procedure yields the following governing differential equations including both quadratic and cubic nonlinear terms for the cracked FGM rectangular plate:

$$p_{10}\ddot{w}_1 + g_{10}w_1 + g_{11}w_1w_2 + g_{12}w_1^2 + g_{13}w_2^2 + g_{14}w_1^2w_2 + g_{15}w_1w_2^2 + g_{16}w_1^3 + g_{17}w_2^3 = f_1\cos\Omega t, \tag{14a}$$

$$p_{20}\ddot{w}_2 + g_{20}w_2 + g_{21}w_1w_2 + g_{22}w_1^2 + g_{23}w_2^2 + g_{24}w_1^2w_2 + g_{25}w_1w_2^2 + g_{26}w_1^3 + g_{27}w_2^3 = f_2\cos\Omega t, \tag{14b}$$

where f_1, f_2 are the magnitudes of the forcing functions, and

$$p_{10} = \frac{I_0ab^2}{4}\sin\left(\frac{a_1\pi}{a}\right)\cos\left(\frac{a_1\pi}{a}\right) + \frac{I_0ba^2}{2\pi a_1}\delta_{21}\cos\left(\frac{\pi a_1}{a-a_1}\right)\sin\left(\frac{\pi a}{a-a_1}\right), \tag{15a}$$

$$p_{20} = I_0b\left\{\frac{1}{4\pi}\left[\pi a_1 + a\cos\left(\frac{a_1\pi}{a}\right)\sin\left(\frac{a_1\pi}{a}\right)\right] + \delta_{23}\sin\left(\frac{\pi a}{a-a_1}\right)\cos\left(\frac{\pi a_1^2}{a(a-a_1)}\right)\right\}. \tag{15b}$$

The lengthy expressions of constants g_{ij} $(i = 1, 2;\ j = 0, \ldots, 7)$ that are nonlinearly dependent on δ_{11}, δ_{13}, δ_{21} and δ_{23} are not given here for brevity.

3 Solution methods

Equation (14) can be used to study the linear and nonlinear free vibration and nonlinear transient response of the cracked FGM plate under a transverse excitation force. If the nonlinear terms and the forcing excitation terms are neglected, (14) reduces to a classical linear free-vibration equation system:

$$p_{10}\ddot{w}_1 + g_{10}w_1 = 0, \tag{16a}$$

$$p_{20}\ddot{w}_2 + g_{20}w_2 = 0, \tag{16b}$$

from which the first two linear natural frequencies can be obtained through a standard solution procedure.

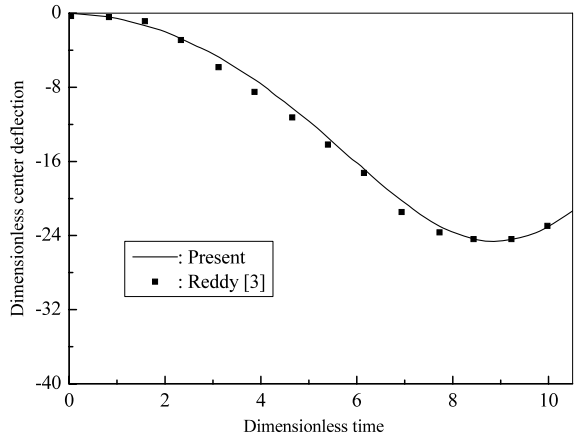

Fig. 2 Temporal evolution curve of center deflection of a simply supported FGM square plate under a suddenly applied uniform load: Comparison with the finite element results [3]

For nonlinear free vibration, our attention is focused on the nonlinear fundamental frequency due to its great importance in determining the dynamic response of the plate. Hence, the terms related to the second-order vibration mode w_2 can be neglected and (14) becomes

$$p_{10}\ddot{w}_1 + g_{10}w_1 + g_{12}w_1^2 + g_{16}w_1^3 = 0. \tag{17}$$

Introducing scale transformation

$$w_1 \to \frac{1}{g_{10}}x_1 \tag{18}$$

and substituting it into (17), yields

$$p_{10}\ddot{x}_1 + g_{10}x_1 + \frac{g_{12}}{g_{10}}x_1^2 + \frac{g_{16}}{g_{10}^2}x_1^3 = 0. \tag{19}$$

This is a nonlinear free-vibration equation with a small perturbation parameter $1/g_{10}$. The nonlinear frequency of the plate with a surface crack can be expressed as [5]

$$\omega_{NL} = \sqrt{\frac{g_{10}}{p_{10}}\left(1 + \frac{9g_{16}g_{10} - 10g_{12}^2}{12g_{10}^2}A^2\right)}, \tag{20}$$

where $A = w_{\max}/h$ and $w_{\max}$ is the deflection amplitude at plate center $(x = b/2, y = a/2)$.

The nonlinear transient response of the surface-cracked FGM plate can be solved from (14) by using Runge–Kutta method.

Table 1 First two dimensionless linear frequencies of intact FGM plates

E_2/E_1	$a/h = 10$		$a/h = 5$	
	$\bar{\omega}_1$	$\bar{\omega}_2$	$\bar{\omega}_1$	$\bar{\omega}_2$
0.2	0.3591	0.6971	0.3987	0.9316
2.0	0.3680	0.7287	0.4089	0.9564
5.0	0.3578	0.7350	0.4142	0.9880

4 Numerical results and discussions

Before proceeding to the nonlinear vibration analysis of simply supported surface-cracked FGM plates, a comparison example is first solved to validate the present analysis. The transient response results are compared in Fig. 2 with the finite element solutions provided by Reddy [3], where the temporal evolution curves of center deflection are presented for a simply supported intact aluminum-zirconia FGM square plate ($a = b = 0.2$ m, $h = 0.01$ m, $n = 2.0$) under a suddenly applied uniform load of intensity of $q_0 = 1$ MPa. The material composition is assumed to follow a simple power-law distribution through the thickness direction such that the plate is 100% zirconia ($E_t = 151$ GPa, $\rho_t = 3000$ kg/m^3) at the top surface and 100% aluminum ($E_b = 70$ GPa, $\rho_b = 2707$ kg/m^3) at the bottom surface. Poisson's ratio is taken as $\nu = 0.3$. The dimensionless center deflection and dimensionless time are defined as $w_c E_b h/(q_0 a^2)$ and $t\sqrt{E_b/(\rho_b a^2)}$, respectively. Our results agree well with the finite element results.

Unless stated otherwise, it is assumed in the following computations that the geometric and material parameters of the rectangular FGM plates are $a/b = 3$, $a = 0.18$ m and $h = 0.018$ m, the Young's modulus ratio $E_2/E_1 = 0.2, 2.0$ and 5.0 where E_1 and E_2 denote the Young's modulus at the top and bottom surfaces of the plate respectively. The top surface of the plate is pure aluminum with material properties: $E_1 = 70 \times 10^9$, $\rho_1 = 2707$ kg/m^3, $\nu = 0.3$. The natural frequency is normalized to be $\bar{\omega}_i = \omega_i \sqrt{ab\rho_1/E_1}/\pi^2$.

Table 1 lists the first two dimensionless linear natural frequencies of simply supported FGM plates ($E_2/E_1 = 0.2, 2.0, 5.0$; $a/h = 5, 10$) without any crack defects. These results can be used to calculate the linear fundamental frequencies of cracked FGM plates from the data given in Fig. 3 where linear fundamental frequency ratios ω/ω_0 are given for FGM plates containing a surface crack of depth $h_1/h = 0.1, 0.2$ at different locations. Here, ω_0 refers to the fundamental frequency of an intact FGM plate. The frequency ratio versus crack location curves are seen to be symmetric due to the geometrically symmetric structure of the plate. The presence of the crack results in a reduced fundamental frequency, i.e. $\omega/\omega_0 \leq 1.0$. The frequency ratio reaches its minimum value when the crack is located at centerline ($a_1/a = 0.5$). It also tends to be lower as the Young's modulus ratio E_2/E_1 decreases from 5.0 to 0.2.

The nonlinear free vibration results, in the form of nonlinear fundamental frequency ratio ω_{NL}/ω_L versus dimensionless center deflection A curves, of various cracked FGM plates are presented in Figs. 4–7, with an intention to investigate the effects of vibration amplitude, crack depth, crack location, the Young's modulus ratio and plate thickness ratio on the nonlinear fundamental frequency of the cracked FGM plate. In these figures, ω_L and ω_{NL} are the linear and the nonlinear fundamental frequency of cracked plates. As can be seen, all cracked FGM plates exhibit typical "hard spring" behavior regardless of the crack depth and crack location.

Figure 4 shows the effect of material property gradient on the nonlinear free vibration behavior of FGM plates with a through-width surface crack ($a_1/a = 0.5$; $h_1/h = 0.1$). The plate with a higher Young's modulus ratio has a higher nonlinear fundamental frequency ratio as dimensionless center deflection A increases up to $A = 0.7$. Beyond this point, the ω_{NL}/ω_L ratio of the plate with $E_2/E_1 = 2.0$ exceeds that of the plate with $E_2/E_1 = 5.0$, indicating that the vibration response of cracked FGM plates does not necessarily change with material property gradient in a monotonic way. This is quite similar to the so-called "non-intermediate" behavior of a nonlinear intact FGM plate that has been reported in [2, 26].

Figure 5 shows the effect of crack depth on the nonlinear free vibration behavior of an FGM plate ($E_2/E_1 = 2.0$) with a through-width surface crack at the centerline of the plate ($a_1/a = 0.5$). It is evident from the results that a deeper surface crack would lead

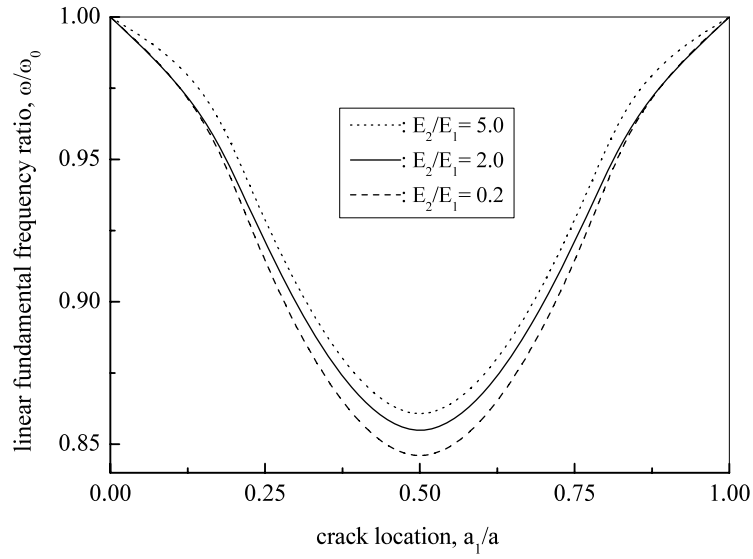

(a) $h_1/h = 0.1$

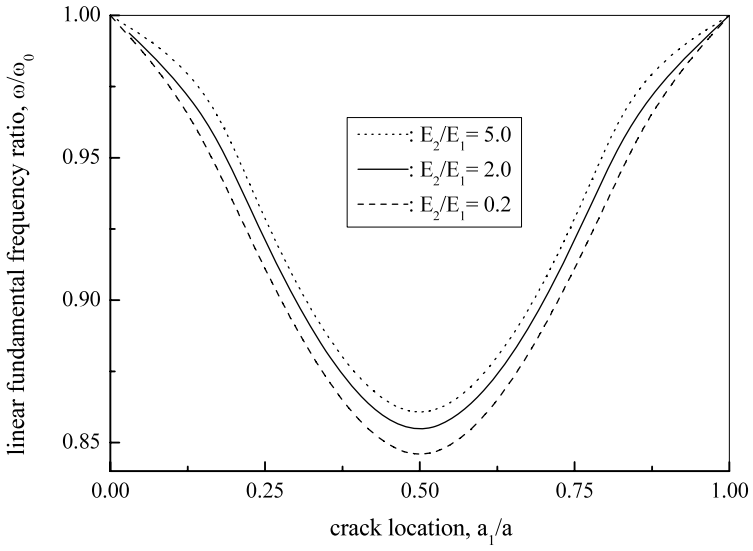

(b) $h_1/h = 0.2$

Fig. 3 Linear fundamental frequency ratio of FGM plates with a through-width surface crack at varying locations: (**a**) $h_1/h = 0.1$; (**b**) $h_1/h = 0.2$

to a lower nonlinear fundamental frequency ratio. This is due to the fact that the plate with a deeper surface crack has a weaker cracked section; thus its stiffness is lower.

The effect of crack location is shown in Fig. 6 where the results for an FGM plate ($E_2/E_1 = 2.0$) with a through-width surface crack ($h_1/h = 0.2$) at different locations are compared. The nonlinear fundamental frequency ratio becomes slightly higher as the crack deviates away from the centerline. This finding is consistent with the results reported previously for cracked FGM beams [19–21].

Apart from material property gradient and crack parameters that have been discussed above, the nonlinear free vibration behavior of cracked FGM plates is found to be influenced by plate thickness ratio as well. This can be clearly observed from Fig. 7 which displays the results for plates with $a/h = 5$ and 10. The nonlinear fundamental frequency ratio of a thinner cracked FGM plate ($a/h = 10$) increases steadily as dimen-

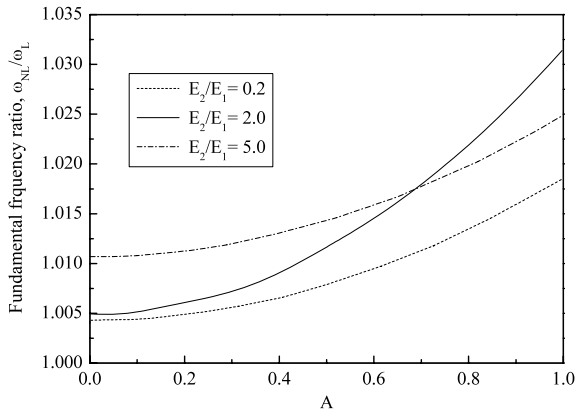

Fig. 4 Nonlinear vibration amplitude–frequency ratio curves of FGM plates with a through-width surface crack ($a_1/a = 0.5;\ h_1/h = 0.1$): Effect of the Young's modulus ratio

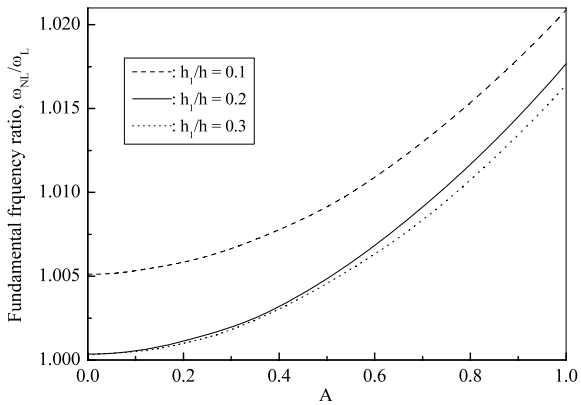

Fig. 5 Nonlinear vibration amplitude–frequency ratio curves of an FGM plate ($E_2/E_1 = 2.0$) with a through-width surface crack ($a_1/a = 0.5$): Effect of crack depth

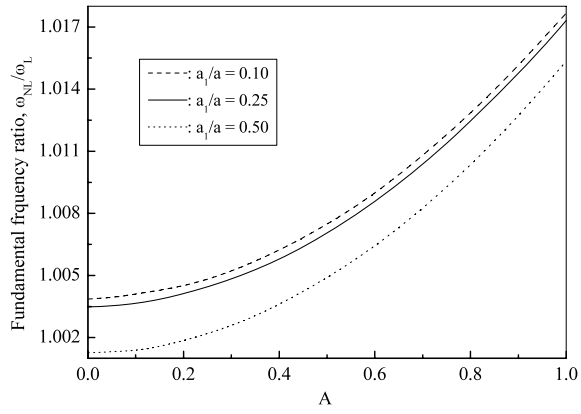

Fig. 6 Nonlinear vibration amplitude–frequency ratio curves of an FGM plate ($E_2/E_1 = 2.0$) with a through-width surface crack ($h_1/h = 0.2$): Effect of crack location

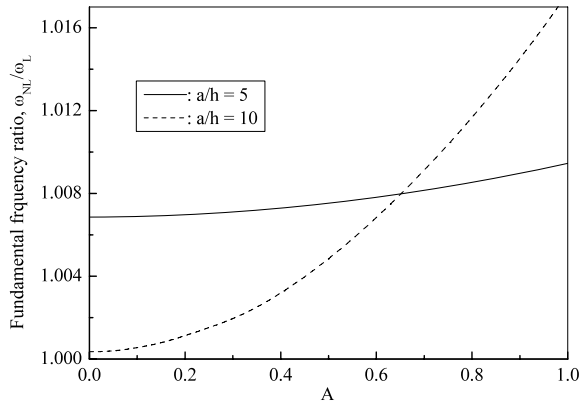

Fig. 7 Nonlinear vibration amplitude–frequency ratio curves of an FGM plate ($E_2/E_1 = 2.0$) with a through-width surface crack ($a_1/a = 0.5;\ h_1/h = 0.2$): Effect of thickness ratio

sionless center deflection increases, whereas that of a thicker plate ($a/h = 5$) only increases slightly.

We further consider the nonlinear transient response of cracked FGM plates subjected to a suddenly applied uniform lateral load. The temporal evolution curves of dimensionless dynamic center deflection $\bar{w} = wE_1h/(q_0a^2)$ versus dimensionless time $t\sqrt{E_1/(\rho_1 a^2)}$ of plates with various parameters are provided in Figs. 8–11. The load intensity is assumed to be $q_0 = 1$ MPa, except in Fig. 11.

Presented in Fig. 8 are the temporal evolution curves of cracked FGM plates with different Young's modulus ($E_2/E_1 = 0.2, 2.0, 5.0$) containing a through-width surface crack ($a_1/a = 0.5;\ h_1/h = 0.1$). The dynamic deflection becomes remarkably higher as the Young's modulus decreases from 5.0 to 0.2. This is because the plate with $E_2/E_1 = 0.2$ has the lowest stiffness among the three considered.

Figure 9 compares the nonlinear transient responses of both intact and cracked FGM plates ($E_2/E_1 = 2.0,\ a_1/a = 0.5$) with different crack depths. As expected, the dynamic deflection is the minimal for the intact plate and increases with an increase in the crack depth which also affects the shape of the nonlinear response curve.

Figure 10 gives the nonlinear transient responses of cracked FGM plates with thickness ratio $a/h = 5$ and 10. The results of their intact counterparts are also provided for direct comparison. The thicker plate ($a/h = 5$) produces much smaller deflection than the thinner one ($a/h = 10$). Also, the intact plate is stiffer

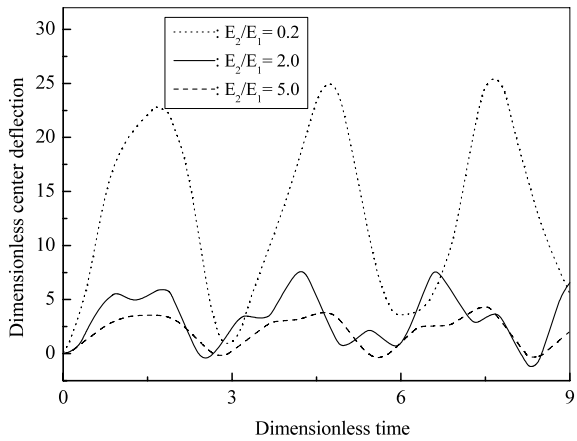

Fig. 8 Temporal evolution curves of center deflection of FGM plates with a through-width surface crack ($a_1/a = 0.5;\ h_1/h = 0.1$): Effect of the Young's modulus ratio

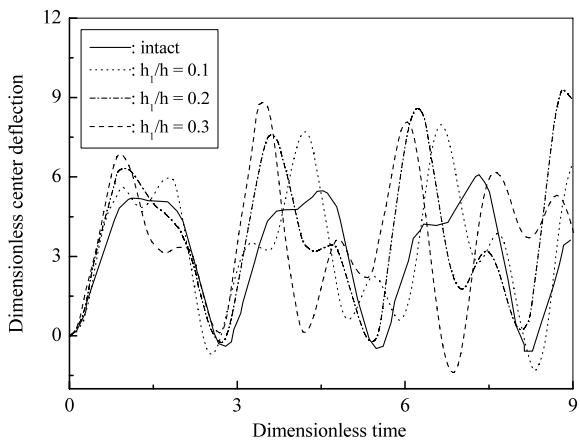

Fig. 9 Temporal evolution curves of center deflection of an FGM plate ($E_2/E_1 = 2.0$) with a through-width surface crack ($a_1/a = 0.5$): Effect of crack depth

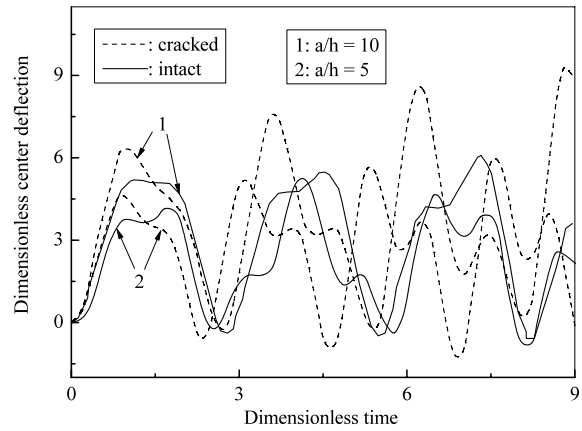

Fig. 10 Temporal evolution curves of center deflection of an FGM plate ($E_2/E_1 = 2.0$) with a through-width surface crack ($a_1/a = 0.5, h_1/h = 0.2$): Effect of thickness ratio

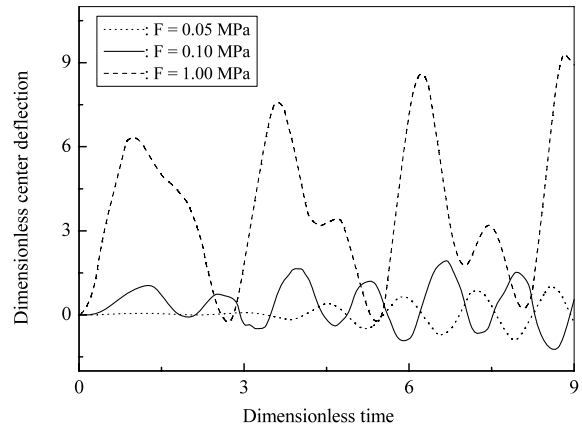

Fig. 11 Temporal evolution curves of center deflection of an FGM plate ($E_2/E_1 = 2.0$) with a through-width surface crack ($a_1/a = 0.5, h_1/h = 0.2$): Effect of load intensity

and stronger than the cracked plate and hence has lower deflections. This effect tends to be more obvious and pronounced for thinner plates. It should be noted that the presence of surface crack not only increases the deflection but also changes the shape of the response curve.

The nonlinear transient responses of a cracked FGM plate ($E_2/E_1 = 2.0$) with a centrally located through-width surface crack ($a_1/a = 0.5,\ h_1/h = 0.2$) under different load intensities are considered in Fig. 11. As can be expected, higher load intensity leads to larger bending deformation of the plate. The nonlinearity can be clearly observed from the results showing that the deflection increase is not linearly proportional to the load increase. Moreover, the shape of transient response curve is seen to be different at different load intensities.

5 Conclusions

The nonlinear vibration behavior of a simply supported, transversely excited functionally graded rectangular plate containing a through-width surface crack has been investigated based on Reddy's third-order shear deformation plate theory, von Karman nonlinear kinematics and rotational spring model.

The material properties vary exponentially along plate thickness direction. The cracked plate is modeled as two sub-plates connected by the rotational spring at the cracked section. The nonlinear governing equations are transformed into a two-degree-of-freedom nonlinear system by using the assumed displacement functions and the Galerkin's method. Linear and nonlinear free vibrations and nonlinear transient response of cracked FGM plates have been discussed in detail. Numerical results show that compared with their intact counterparts, cracked FGM plates have lower natural frequencies and larger deflections. The natural frequency and nonlinear fundamental frequency ratio become lower whereas dynamic deflection increases as the crack depth increases and the Young's modulus decreases. The effect of crack location is relatively smaller but does reduce both linear and nonlinear fundamental frequency ratios and increase the dynamic deflection as the crack location moves closer to the centerline of the plate. Furthermore, the "non-intermediate" behavior is also observed in cracked FGM plates at large vibration amplitudes.

Appendix

In governing equation (5), the nonlinear and linear partial differential operators L_{jL} and L_{jR} $(j = 1, \ldots, 5)$ take the form of

$$\begin{aligned} L_{1L} = {} & A_{11}\frac{\partial^2 u_0^i}{\partial x^2} + A_{66}\frac{\partial^2 u_0^i}{\partial y^2} + (A_{12}+A_{66})\frac{\partial^2 v_0^i}{\partial x\,\partial y} + (B_{11}+c_1E_{11})\frac{\partial^2 \phi_x^i}{\partial x^2} + (B_{66}+c_1E_{66})\frac{\partial^2 \phi_x^i}{\partial y^2} \\ & + (B_{12}-c_1E_{12}+B_{66}-c_1E_{66})\frac{\partial^2 \phi_y^i}{\partial x\,\partial y} + A_{11}\frac{\partial w_0^i}{\partial x}\frac{\partial^2 w_0^i}{\partial x^2} + A_{66}\frac{\partial w_0^i}{\partial x}\frac{\partial^2 w_0^i}{\partial y^2} + (A_{12}+A_{66})\frac{\partial w_0^i}{\partial y}\frac{\partial^2 w_0^i}{\partial x\,\partial y} \\ & - c_1E_{11}\frac{\partial^3 w_0^i}{\partial x^3} - c_1(E_{12}+2E_{66})\frac{\partial^3 w_0^i}{\partial x\,\partial y^2}, \end{aligned} \tag{A.1}$$

$$L_{1R} = I_0\ddot{u}_0^i + (I_1 - c_1I_3)\ddot{\phi}_x^i - c_1I_3\frac{\partial \ddot{w}_0^i}{\partial x}, \tag{A.2}$$

$$\begin{aligned} L_{2L} = {} & A_{66}\frac{\partial^2 v_0^i}{\partial x^2} + A_{22}\frac{\partial^2 v_0^i}{\partial y^2} + (A_{21}+A_{66})\frac{\partial^2 u_0^i}{\partial x\,\partial y} + (B_{66}+c_1E_{66})\frac{\partial^2 \phi_y^i}{\partial x^2} + (B_{22}+c_1E_{22})\frac{\partial^2 \phi_y^i}{\partial y^2} \\ & + (B_{21}-c_1E_{21}+B_{66}-c_1E_{66})\frac{\partial^2 \phi_x^i}{\partial x\,\partial y} + A_{66}\frac{\partial w_0^i}{\partial y}\frac{\partial^2 w_0^i}{\partial x^2} + A_{22}\frac{\partial w_0^i}{\partial y}\frac{\partial^2 w_0^i}{\partial y^2} \\ & + (A_{21}+A_{66})\frac{\partial w_0^i}{\partial x}\frac{\partial^2 w_0^i}{\partial x\,\partial y} - c_1E_{22}\frac{\partial^3 w_0^i}{\partial y^3} - c_1(E_{12}+2E_{66})\frac{\partial^3 w_0^i}{\partial x^2\,\partial y}, \end{aligned} \tag{A.3}$$

$$L_{2R} = I_0\ddot{v}_0^i + (I_1 - c_1I_3)\ddot{\phi}_y^i - c_1I_3\frac{\partial \ddot{w}_0^i}{\partial y}, \tag{A.4}$$

$$\begin{aligned} L_{3L} = {} & A_{21}\frac{\partial u_0^i}{\partial x}\frac{\partial^2 w_0^i}{\partial y^2} + A_{11}\frac{\partial u_0^i}{\partial x}\frac{\partial^2 w_0^i}{\partial x^2} + 2A_{66}\frac{\partial u_0^i}{\partial y}\frac{\partial^2 w_0^i}{\partial x\,\partial y} + (A_{21}+A_{66})\frac{\partial^2 u_0^i}{\partial x\,\partial y}\frac{\partial w_0^i}{\partial y} + A_{11}\frac{\partial^2 u_0^i}{\partial x^2}\frac{\partial w_0^i}{\partial x} \\ & + A_{66}\frac{\partial^2 u_0^i}{\partial y^2}\frac{\partial w_0^i}{\partial x} + c_1E_{11}\frac{\partial^3 u_0^i}{\partial x^3} + c_1(E_{21}+2E_{66})\frac{\partial^3 u_0^i}{\partial x\,\partial y^2} + 2A_{66}\frac{\partial v_0^i}{\partial x}\frac{\partial^2 w_0^i}{\partial x\,\partial y} + A_{22}\frac{\partial v_0^i}{\partial y}\frac{\partial^2 w_0^i}{\partial y^2} \\ & + A_{12}\frac{\partial v_0^i}{\partial y}\frac{\partial^2 w_0^i}{\partial x^2} + A_{22}\frac{\partial^2 v_0^i}{\partial y^2}\frac{\partial w_0^i}{\partial y} + A_{66}\frac{\partial^2 v_0^i}{\partial x^2}\frac{\partial w_0^i}{\partial y} + (A_{12}+A_{66})\frac{\partial^2 v_0^i}{\partial x\,\partial y}\frac{\partial w_0^i}{\partial x} + c_1E_{22}\frac{\partial^3 v_0^i}{\partial y^3} \\ & + c_1(E_{12}+2E_{66})\frac{\partial^3 v_0^i}{\partial y\,\partial x^2} + \left(A_{55}+c_2^2F_{55}-2c_2D_{55}\right)\frac{\partial^2 w_0^i}{\partial x^2} + \left(A_{44}+c_2^2F_{44}-2c_2D_{44}\right)\frac{\partial^2 w_0^i}{\partial y^2} \end{aligned}$$

$$
\begin{aligned}
&+2c_1(E_{66}-E_{12})\frac{\partial^2 w_0^i}{\partial x^2}\frac{\partial^2 w_0^i}{\partial y^2}+2c_1E_{66}\frac{\partial^2 w_0^i}{\partial x\,\partial y}\frac{\partial^2 w_0^i}{\partial y^2}+2c_1(E_{21}-2E_{66})\left(\frac{\partial^2 w_0^i}{\partial x\,\partial y}\right)^2\\
&+2(A_{21}+2A_{66})\frac{\partial w_0^i}{\partial x}\frac{\partial^2 w_0^i}{\partial x\,\partial y}\frac{\partial w_0^i}{\partial y}+\frac{3}{2}A_{22}\left(\frac{\partial w_0^i}{\partial y}\right)^2\frac{\partial^2 w_0^i}{\partial y^2}+\left(\frac{1}{2}A_{21}+A_{66}\right)\left(\frac{\partial w_0^i}{\partial x}\right)^2\frac{\partial^2 w_0^i}{\partial y^2}\\
&+\left(A_{66}+\frac{1}{2}A_{21}\right)\left(\frac{\partial w_0^i}{\partial y}\right)^2\frac{\partial^2 w_0^i}{\partial x^2}+\frac{3}{2}A_{11}\left(\frac{\partial w_0^i}{\partial x}\right)^2\frac{\partial^2 w_0^i}{\partial x^2}-c_1^2H_{11}\frac{\partial^4 w_0^i}{\partial x^4}\\
&-c_1^2H_{22}\frac{\partial^4 w_0^i}{\partial y^4}-2c_1^2(H_{21}-2H_{66})\frac{\partial^4 w_0^i}{\partial x^2\,\partial y^2}+\left(-2c_2D_{55}+c_2^2F_{55}+A_{55}\right)\frac{\partial\phi_x^i}{\partial x}\\
&+(B_{21}-c_1E_{21})\frac{\partial\phi_x^i}{\partial x}\frac{\partial^2 w_0^i}{\partial y^2}+2(B_{66}-c_1E_{66})\frac{\partial\phi_x^i}{\partial y}\frac{\partial^2 w_0^i}{\partial x\,\partial y}+(B_{21}+B_{66}-c_1E_{21}-c_1E_{66})\frac{\partial^2\phi_x^i}{\partial x\,\partial y}\frac{\partial w_0^i}{\partial y}\\
&+(B_{11}-c_1E_{11})\frac{\partial^2\phi_x^i}{\partial x^2}\frac{\partial w_0^i}{\partial x}+(B_{11}-c_1E_{11})\frac{\partial\phi_x^i}{\partial x}\frac{\partial^2 w_0^i}{\partial x^2}+(B_{66}-c_1E_{66})\frac{\partial^2\phi_x^i}{\partial y^2}\frac{\partial w_0^i}{\partial x}\\
&+\left(c_1F_{11}-c_1^2H_{11}\right)\frac{\partial^3\phi_x^i}{\partial x^3}+c_1(F_{21}+2F_{66}-c_1H_{21}-2c_1H_{66})\frac{\partial^3\phi_x^i}{\partial x\,\partial y^2}\\
&+\left(-2c_2D_{44}+A_{44}+c_2^2F_{44}\right)\frac{\partial\phi_y^i}{\partial y}+(B_{22}-c_1E_{22})\frac{\partial\phi_y^i}{\partial y}\frac{\partial^2 w_0^i}{\partial y^2}+2(B_{66}-c_1E_{66})\frac{\partial\phi_y^i}{\partial x}\frac{\partial^2 w_0^i}{\partial x\,\partial y}\\
&+(B_{66}-c_1E_{66})\frac{\partial^2\phi_y^i}{\partial x^2}\frac{\partial w_0^i}{\partial y}+(B_{12}-c_1E_{12})\frac{\partial\phi_y^i}{\partial y}\frac{\partial^2 w_0^i}{\partial x^2}+(B_{22}-c_1E_{22})\frac{\partial^2\phi_y^i}{\partial y^2}\frac{\partial w_0^i}{\partial y}\\
&+(B_{12}+B_{66}-c_1E_{12}-c_1E_{66})\frac{\partial^2\phi_y^i}{\partial x\,\partial y}\frac{\partial w_0^i}{\partial x}+\left(c_1F_{22}-c_1^2H_{22}\right)\frac{\partial^3\phi_y^i}{\partial y^3}\\
&+c_1(F_{12}+2F_{66}-c_1H_{12}-2c_1H_{66})\frac{\partial^3\phi_y^i}{\partial x^2\,\partial y}+F\cos\Omega_1 t,
\end{aligned}
\tag{A.5}
$$

$$
L_{3R}=I_0\ddot{w}_0^i-c_1^2I_6\left(\frac{\partial^2\ddot{w}_0^i}{\partial x^2}+\frac{\partial^2\ddot{w}_0^i}{\partial y^2}\right)+c_1I_3\left(\frac{\partial\ddot{u}_0^i}{\partial x}+\frac{\partial\ddot{v}_0^i}{\partial y}\right)+c_1(I_4-c_1I_6)\left(\frac{\partial\ddot{\phi}_x^i}{\partial x}+\frac{\partial\ddot{\phi}_y^i}{\partial y}\right),
\tag{A.6}
$$

$$
\begin{aligned}
L_{4L}=&(B_{11}-c_1E_{11})\frac{\partial^2 u_0^i}{\partial x^2}+(B_{66}-c_1E_{66})\frac{\partial^2 u_0^i}{\partial y^2}+(B_{12}+B_{66}-c_1E_{12}-c_1E_{66})\frac{\partial^2 v_0^i}{\partial x\,\partial y}\\
&+(B_{11}-c_1E_{11})\frac{\partial w_0^i}{\partial x}\frac{\partial^2 w_0^i}{\partial x^2}+(B_{12}+B_{66}-c_1E_{12}-c_1E_{66})\frac{\partial w_0^i}{\partial y}\frac{\partial^2 w_0^i}{\partial x\,\partial y}+(B_{66}-c_1E_{66})\frac{\partial w_0^i}{\partial x}\frac{\partial^2 w_0^i}{\partial y^2}\\
&+\left(-c_1F_{11}+c_1^2H_{11}\right)\frac{\partial^3 w_0^i}{\partial x^3}+c_1(-F_{12}-2F_{66}+c_1H_{12}+2c_1H_{66})\frac{\partial^3 w_0^i}{\partial x\,\partial y^2}\\
&-\left(A_{55}-2c_2D_{55}+c_2^2F_{55}\right)\frac{\partial w_0^i}{\partial x}+\left(D_{11}-2c_1F_{11}+c_1^2H_{11}\right)\frac{\partial^2\phi_x^i}{\partial x^2}+\left(D_{66}-2c_1F_{66}+c_1^2H_{66}\right)\frac{\partial^2\phi_x^i}{\partial y^2}\\
&+\left(D_{12}-2c_1F_{12}-2c_1F_{66}+D_{66}+c_1^2H_{12}+c_1^2H_{66}\right)\frac{\partial^2\phi_y^i}{\partial x\,\partial y}-\left(A_{55}-2c_2D_{55}+c_2^2F_{55}\right)\phi_x^i,
\end{aligned}
\tag{A.7}
$$

$$
L_{4R}=\left(I_1-c_1I_3\right)\ddot{u}_0^i+\left(I_2-2c_1I_4+c_1^2I_6\right)\ddot{\phi}_x^i-c_1(I_4-c_1I_6)\frac{\partial\ddot{w}_0^i}{\partial x},
\tag{A.8}
$$

$$
L_{5L}=(B_{66}-c_1E_{66})\frac{\partial^2 v_0^i}{\partial x^2}+(B_{22}-c_1E_{22})\frac{\partial^2 v_0^i}{\partial y^2}+(B_{21}+B_{66}-c_1E_{21}-c_1E_{66})\frac{\partial^2 u_0^i}{\partial x\,\partial y}
$$

$$+ (B_{66} - c_1 E_{66}) \frac{\partial w_0^i}{\partial y} \frac{\partial^2 w_0^i}{\partial x^2} + (B_{22} - c_1 E_{22}) \frac{\partial w_0^i}{\partial y} \frac{\partial^2 w_0^i}{\partial y^2} + (B_{21} + B_{66} - c_1 E_{21} - c_1 E_{66}) \frac{\partial w_0^i}{\partial x} \frac{\partial^2 w_0^i}{\partial x \, \partial y}$$

$$+ \left(-c_1 F_{22} + c_1^2 H_{22}\right) \frac{\partial^3 w_0^i}{\partial y^3} + c_1 (-F_{21} - 2F_{66} + c_1 H_{21} + 2c_1 H_{66}) \frac{\partial^3 w_0^i}{\partial x^2 \, \partial y}$$

$$- \left(A_{44} - 2c_2 D_{44} + c_2^2 F_{44}\right) \frac{\partial w_0^i}{\partial y} + \left(D_{66} - 2c_1 F_{66} + c_1^2 H_{66}\right) \frac{\partial^2 \phi_y^i}{\partial x^2}$$

$$+ \left(D_{22} - 2c_1 F_{22} + c_1^2 H_{22}\right) \frac{\partial^2 \phi_y^i}{\partial y^2} + \left(D_{21} - 2c_1 F_{21} - 2c_1 F_{66} + D_{66} + c_1^2 H_{21} + c_1^2 H_{66}\right) \frac{\partial^2 \phi_x^i}{\partial x \, \partial y}$$

$$- \left(A_{44} - 2c_2 D_{44} + c_2^2 F_{44}\right) \phi_y^i, \tag{A.9}$$

$$L_{5R} = (I_1 - c_1 I_3) \ddot{v}_0 + \left(I_2 - 2c_1 I_4 + c_1^2 I_6\right) \ddot{\phi}_y^i - c_1 (I_4 - c_1 I_6) \frac{\partial \ddot{w}_0^i}{\partial y}, \tag{A.10}$$

where $c_2 = 3c_1$.

References

1. Ichikawa, K. (ed.): Functionally Graded Materials in the 21st Century: A Workshop on Trends and Forecasts. Kluwer Academic, Norwell (2000)
2. Praveen, G.N., Reddy, J.N.: Nonlinear transient thermoelastic analysis of functionally graded ceramic-metal plates. Int. J. Solids Struct. **35**(33), 4457–4476 (1998)
3. Reddy, J.N.: Analysis of functionally graded plates. Int. J. Numer. Methods Eng. **47**(1–3), 663–684 (2000)
4. Yang, J., Kitipomchai, S., Liew, K.M.: Large-amplitude vibration of thermo-electromechanically stressed FGM laminated plates. Comput. Methods Appl. Mech. Eng. **192**(35–36), 861–3885 (2003)
5. Huang, X.L., Shen, H.S.: Nonlinear vibration and dynamic response of functionally graded plates in thermal environments. Int. J. Solids Struct. **41**(9–10), 2403–2407 (2004)
6. Chen, C.S.: Nonlinear vibration of a shear deformable functionally graded plate. Compos. Struct. **68**(3), 295–302 (2005)
7. Kitipornchai, S., Yang, J., Liew, K.M.: Semi-analytical solution for nonlinear vibration of laminated FGM plates with geometric imperfections. Int. J. Solids Struct. **41**(9–10), 2235–2257 (2004)
8. Yang, J., Huang, X.L.: Nonlinear transient response of functionally graded plates with general imperfections in thermal environments. Comput. Methods Appl. Mech. Eng. **196**(25–28), 2619–2630 (2007)
9. Dimarogonas, A.D.: Vibration of cracked structures: a state-of-the-art review. Eng. Fract. Mech. **55**(5), 831–857 (1996)
10. Jin, Z.H., Noda, N.: Crack–tip singular fields in nonhomogeneous materials. ASME J. Appl. Mech. **61**, 738–740 (1994)
11. Erdogan, F., Wu, B.H.: The surface crack problem for a plate with functionally graded properties. ASME J. Appl. Mech. **64**(3), 449–456 (1997)
12. Jin, Z.H., Paulino, G.H.: Transient thermal stress analysis of an edge crack in a functionally graded material. Int. J. Fract. **107**(1), 73–98 (2001)
13. Delale, F., Erdogan, F.: The crack problem for a nonhomogeneous plane. ASME J. Appl. Mech. **50**(3), 609–614 (1983)
14. Abanto-Bueno, J., Lambros, J.: Parameters controlling fracture resistance in functionally graded materials under mode I loading. Int. J. Solids Struct. **43**(13), 3920–3939 (2006)
15. Wang, B.L., Noda, N.: Thermally induced fracture of a smart functionally graded composite structure. Theor. Appl. Fract. Mech. **35**(2), 93–109 (2001)
16. Guo, L.C., Wu, L.Z., Zeng, T., Ma, L.: The dynamic fracture behavior of a functionally graded coating–substrate system. Compos. Struct. **64**(3–4), 433–441 (2004)
17. Sridhar, R., Chakraborty, A., Gopalakrishnan, S.: Wave propagation analysis in anisotropic and inhomogeneous uncracked and cracked structures using pseudospectral finite element method. Int. J. Solids Struct. **43**(16), 4997–5031 (2006)
18. Birman, V., Byrd, L.W.: Vibration of damaged cantilevered beams manufactured from functionally graded materials. AIAA J. **45**, 2747–2757 (2007)
19. Yang, J., Chen, Y.: Free vibration and buckling analyses of functionally graded beams with edge cracks. Compos. Struct. **83**(1), 48–60 (2008)
20. Yang, J., Chen, Y., Xiang, Y., Jia, X.L.: Free and forced vibration of cracked inhomogeneous beams under an axial force and a moving load. J. Sound Vib. **312**(1–2), 166–181 (2008)
21. Ke, L.L., Yang, J., Kitipornchai, S., Xiang, Y.: Flexural vibration and elastic buckling of a cracked Timoshenko beam made of functionally graded materials. Mech. Adv. Mater. Struct. (2009, in press)
22. Reddy, J.N.: Mechanics of Laminated Composite Plates and Shells: Theory and Analysis. CRC Press, New York (2004)

23. Broek, D.: Elementary Engineering Fracture Mechanics. Nijhoff, Dordrecht (1986)
24. Bhimaraddi, A.: Large-amplitude vibrations of imperfect antisymmetric angle-ply laminated plates. J. Sound Vib. **162**(3), 457–470 (1997)
25. Nosir, A., Reddy, J.N.: A study of non-linear dynamic equations of higher-order deformation plate theories. Int. J. Non-Linear Mech. **26**(2), 233–249 (1991)
26. Yang, J., Kitipomchai, S., Liew, K.M.: Non-linear analysis of the thermo-electromechanical behaviour of shear deformable FGM plates with piezoelectric actuators. Int. J. Numer. Methods Eng. **59**(12), 1605–1632 (2004)